Reproducibility of Fluorine-18-6-Fluorodopa Positron Emission Tomography in Normal Human Subjects

François J.G. Vingerhoets, Barry J. Snow, Michael Schulzer, Scott Morrison, Thomas J. Ruth, James E. Holden, Sandra Cooper and Donald B. Calne

Neurodegenerative Disorders Centre and TRIUMF, University of British Columbia, Vancouver, British Columbia; and Department of Medical Physics, University of Wisconsin; Madison, Wisconsin

Fluorine-18-6-fluorodopa (FD) positron emission tomography (PET) is established for measuring nigrostriatal dopaminergic function. This is despite the absence of data on the reproducibility of results. **Methods:** With an ECAT 953B/31 tomograph, we performed two or three repeated FD PET scans in 10 normal subjects to measure the scan-to-scan variation in the total striatal uptake rate constant (Ki). **Results:** We found a scan-to-scan standard deviation (s.d.) of 8.7% of the mean. The between-subject s.d. was 26% of the mean, resulting in a reliability coefficient of 90%. Analysis of the variation in the components contributing to Ki showed a reliability varying from 77% to 86% (depending on the different time points analyzed) for emission data measured by the PET camera. The reliability of the blood radioactivity time course, as reflected by the stretch time, varied from 43% to 81%. The overall reliability for the correction of the blood time course for metabolites of FD was 71%. Variation in the blood radioactivity contributed to the variability of Ki by 50% more than the metabolite correction and by 200% more than the emission data. **Conclusion:** The striatal Ki is a reliable measurement; it has a 95% chance of lying within ±18% of its value for an individual normal subject.

Key Words: fluorodopa; PET imaging

J Nucl Med 1994; 35:18–24

Fluorine-18-6-Fluorodopa (FD) positron emission tomography (PET) is widely used to assess nigrostriatal dopaminergic function. Cross-sectional and longitudinal studies [e.g., on the effects of aging (*1*), medication (*2,3*) and intracerebral transplants (*4–6*)] have been performed with this technique. The significance of changes of the striatal FD uptake rate constant (Ki) depends on the reproducibility of the FD PET results (*7*). This has been reported only in nonhuman primates (*8*). Controversies regarding the place of PET in the clinical assessment of movement disorders have focused on the lack of such data (*9,10*). We performed repeat FD PET scans in normal humans to measure scan-to-scan variation in Ki. We also studied the variations of individual determinants (emission data measured by the PET camera, blood radioactivity and measurements of the peripheral metabolites of FD) and their effects on Ki.

Received Apr. 8, 1993; revision accepted Sept. 27, 1993.

For correspondence or reprints contact: Barry J. Snow, MD, Neurodegenerative Disorders Centre, University Hospital—UBC Site, 2211 Westbrook Mall, Vancouver, BC V6T 2B5, Canada.

SUBJECTS AND METHODS

Subjects

Ten normal subjects (age 31–72 yr, mean 51 yr; 4 males, 6 females) were studied. None had neurologic disease by history or examination. Each subject was scanned twice within 3 wk (average ± s.d., 11.0 ± 5.4 days) and eight were scanned a third time within 2 mo from the first scan (40 ± 14.8 days). Subjects gave written informed consent before each scan. These studies were authorized by the U.B.C. Ethics Committee.

PET

PET studies were performed using an ECAT 953B/31 tomograph (Siemens Canada/CTI, Knoxville, TN). This tomograph permits simultaneous acquisition of 31 axial planes with a center-to-center separation of 3.4 mm and an average 5.5-mm in-plane and 5-mm axial reconstructed resolution, full width at half maximum. Signal variation due to changes in axial position of objects with geometry of the human striatum is minimal in this scanner (*11*). The subject was positioned with the image plane parallel to the orbito-meatal line. A thermo-plastic face mask was molded to restrain head movement and was also used for subsequent scans on a particular subject. Measurements were taken to ensure the subject was in the same position for each scan: (1) the position of the beams from gantry-mounted lasers were recorded on the mask, and (2) the distances from the tips of the upper incisors, the meati of the ears and mandibular angles to the inferior borders of the mask and to the laser-lines were measured. Tissue attenuation was measured with three ^{68}Ge rotating rod sources. Carbidopa (200 mg) was given orally 1 hr before tracer injection. FD (111.1 ± 2.03 MBq) was injected intravenously as a bolus at the beginning of the scan. Twelve 10-min, sequential emission scans were performed starting immediately after injection.

Whole arterial blood samples (2 ml) were obtained from the radial artery using an indwelling catheter as follows: Eight samples were obtained during the first minute beginning during the tracer injection; four were obtained during the next minute; one

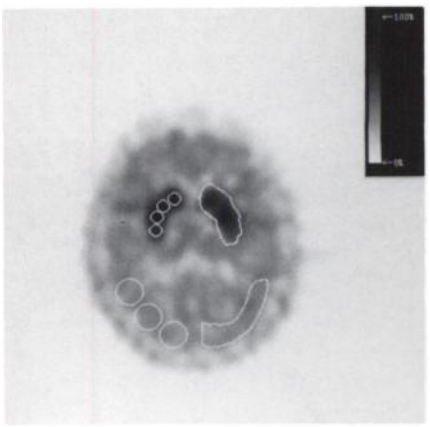

FIGURE 1.
Typical sets of ROIs. (Right) TS method and (Left) CP method.

was obtained at 3, 4, 5, 7, 12 and 17 min; and one was obtained every 10 min from 25 to 115 min. Each sample was centrifuged and total plasma radioactivity was determined on 0.5-ml samples with a well counter. The results were corrected for radioactive decay.

Plasma metabolites of FD were measured from 5-ml samples drawn at 2.5, 5, 7.5, 10, 15, 20, 30, 45, 60, 75, 90 and 120 min. The fractions of FD and 3-O-methyl-FD (3OMFD) were determined by a batch-contact alumina-extraction method (*12*). Each determination was performed twice. A standard deviation of the fraction was calculated of each time point taking into account the variation between the two measurements and the error from the well counter (estimated by Poisson's law). The tomograph was calibrated so that plasma activity and regional brain activity were expressed in the same units.

Each subsequent scan was performed with the same protocol.

Data Analysis

Activity collected from 60 to 120 min after FD administration was summed to produce an integral image. On this image, regions of interest (ROIs) were placed using two different methods as follows.

Total Striatum Set (TS). Two irregular ROIs (930 mm^2 ± 90 mm^2) encompassing the whole striatum were drawn manually on each slice where the striata were visible. The borders corresponded approximately to the threshold of 50% of the peak value of the image (Fig. 1). Two background ROIs (1040 mm^2 ± 150 mm^2) were located on the posterior temporoparietal cortex of the same slices, avoiding the midline and the ventricules (Fig. 1). The four ROIs on each slice were superimposed on the 12 time frames. Total striatal activity measurements were obtained for both the left and right striatum by summing all striatal activity measurements for that side. For the background activity, the activities of both ROIs on all slices were summed and normalized by area to the striatal ROIs.

Caudate and Putamen Set (CP). One circular ROI of 61.2 mm^2 (diameter = 8.8 mm) was positioned by inspection on each caudate nucleus and adjusted on the integral image to maximize the average ROI activity (Fig. 1). Three circular ROIs of 61.2 mm^2 (diameter = 8.8 mm) were placed without overlap along the axis of each putamen and were similarly adjusted (Fig. 1). Three background circular ROIs of 297 mm^2 (diameter = 19.4 mm) were placed on each side on the temporo-parietal cortex (Fig. 1). This was repeated for the five slices where the caudate and the putamen were most clearly seen. The 70 ROIs were replicated over the 12 time frames. For each frame, ROIs of like structures were averaged, culminating in separate measurements for left and right caudate, left and right putamen and background.

Correction for FD and 3OMFD in the striatal signal was performed by subtracting the background from striatal activity (*13*). Results were obtained in Bq/striatum for TS and in Bq/ml for CP.

The same sets of ROIs were used to analyze each scan of a single subject. When necessary, the locations were adjusted to compensate for repositioning.

Tissue and plasma data were analyzed by the graphical method described by Patlak and colleagues (*13–15*). This was performed for both sets of ROIs on data from 20 to 120 min. In addition, for TS, this was performed from 20 to 90 min. A 20–120-min graphical analysis was also performed on the TS using a metabolite correction factor fixed at the study mean.

The scans were also analyzed as a ratio of target-to-background (ratio method) on the integral image using TS. After correction for area of the ROIs, the striatal activity was divided by the background activity.

Statistical Analysis

A one-way ANOVA was performed to estimate the standard deviation between (SDB) and within (SDW) subjects. Confidence intervals for SDW were calculated using chi-squared distribution and the reliability coefficients were estimated (*16*). The reliability coefficient measures the intraclass correlation, i.e., the correlation between two measurements observed in the same individual at different times. It is therefore an indication of the reproducibility of the measurements over time.

The analysis proceeded in a hierarchical manner beginning with Ki and continuing down the components of the graphical analysis to the measurements of emission, metabolite correction and blood radioactivity. The striatal and background activities were divided by the amount of FD injected and multiplied by the weight of the subject to allow inter-subject comparison. To compare with CP, the TS activities were expressed in Bq/ml by averaging the mean activity of each ROI. For metabolite correction, the slopes of the ratio 3OMFD/FD versus time were compared. This function has been shown to be linear (*12, 17, 18*). To test the line fit, a chi-square goodness of fit test for the present data was performed for each analysis. For blood radioactivity, the plasma activity (PA) at individual time points, the area under the curve of plasma activity (IPA) and stretch-time (the ratio θ = IPA/PA) were compared. PA and IPA were corrected for the weight of the subject and amount of FD injected. To simplify analysis of multiple time-related results, data were compared at scan numbers 3, 6, 9 and 12.

To analyze the propagation of the errors of the three sets of data (emission, metabolite correction, blood) on the final result, the graphical analysis was performed on the data of each scan with all the blood sets and all the metabolite corrections for the same subject after correction for the amount of FD injected. An ANOVA was carried out on the final Ki, with subjects as random blocks, and emission, blood and metabolite correction as random effects. Interactions were included in the model. A variance components analysis was then applied to estimate the net contributions of subjects, emission, metabolite correction and blood to the total variability of Ki (*19*).

To examine the mean Ki difference between 20–90 min versus 20–120 min analysis, a weighted estimate was derived across patients with the weight inversely proportional to the variances of the individual means. The significance of the difference was tested by a z-test.

Reliability coefficients were used to evaluate sample size re-

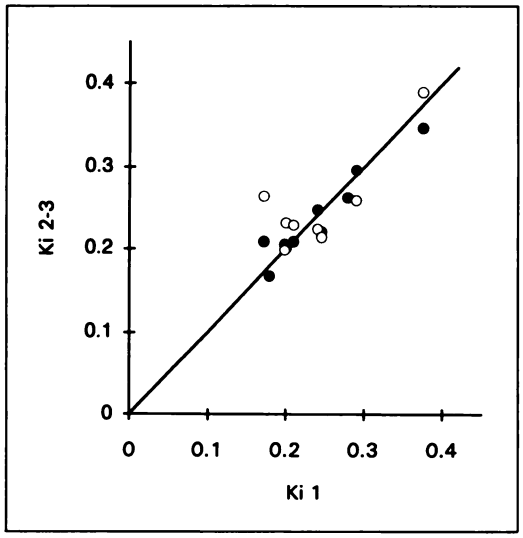

FIGURE 2. Bilateral TS Ki reliability. Ki at scan 2 (●) and scan 3 (○) are plotted against Ki at scan 1. The straight line represents the perfect agreement line for Ki between scan 1 (Ki_1) and scan 2 or 3 (Ki_{2-3}).

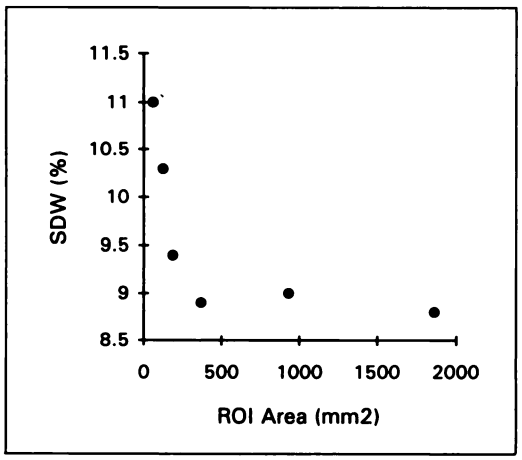

FIGURE 3. Relationship between ROI area and within standard deviation of Ki (SDW). From left to right, the ROIs areas correspond to unilateral caudate, bilateral caudate, unilateral putamen, bilateral putamen, unilateral striatum and bilateral striatum.

quirements for future studies (assuming a parallel group design) (*20*).

RESULTS

Striatal Uptake Constant (Ki)

Ki, using TS from 20 to 120 min, gave a SDW of 8.7% of the group mean value (Fig. 2). The SDB was 26% resulting in a reliability coefficient of 90%. Table 1 shows detailed results of Ki from the two ROI sets and of the ratio method.

When the analysis was restricted to the first 90 min of scanning, the mean Ki from combined TS increased by 3.7% ($p < 0.00005$; $z = 4.08$). The reliability was unchanged at 90% with minimal effects on SDB and SDW (Table 1).

The SDW of the Kis was dependent upon the area of the ROI (Fig. 3), leading to lower reliability with the small ROIs from the CP compared to the TS (Table 1).

There was a significant inverse relationship between Ki and age for the TS (slope: −0.9%/yr, $p = 0.049$) but not for the CP (−0.6%/yr; $p = 0.15$) (Fig. 4). This difference was enhanced by exclusion of the outlier with a high result (TS: −0.7%/yr, $p = 0.01$; CP: −0.4%/yr, $p = 0.13$).

Emission Data

For the TS, the SDW varied between 7.6% and 9.4%, with a SDB from 16% to 18% and the reliability

TABLE 1
Ki Mean Values, Estimates of Standard Deviations and Reliability Coefficients*

	Side	Mean	SDB (% of mean)	SDW (% of mean)	95% CI	R
Graphical TS						
20 to 120 min	Bilateral	2.41	0.64 (26%)	0.21 (8.7%)	(7%–13%)	90%
(10^{-1} ml min^{-1}	Right	2.43	0.61 (25%)	0.22 (9%)	(7%–13%)	89%
$striatum^{-1}$)	Left	2.40	0.68 (28%)	0.22 (9.1%)	(7%–14%)	91%
20–90 min	Bilateral	2.50	0.64 (26%)	0.22 (8.9%)	(7%–14%)	90%
	Right	2.52	0.62 (24%)	0.24 (9.4%)	(7%–15%)	87%
	Left	2.49	0.70 (28%)	0.23 (9.1%)	(7%–15%)	90%
Graphical CP						
Caudate	Bilateral	2.14	0.47 (22%)	0.22 (10.3%)	(8%–15%)	82%
(10^{-2} ml min^{-1} cc^{-1})	Right	2.12	0.46 (22%)	0.23 (10.6%)	(8%–16%)	80%
	Left	2.18	0.49 (22%)	0.25 (11.3%)	(9%–17%)	80%
Putamen	Bilateral	2.02	0.44 (22%)	0.18 (8.9%)	(7%–13%)	85%
(10^{-2} ml min^{-1} cc^{-1})	Right	2.00	0.44 (22%)	0.20 (10.1%)	(8%–15%)	82%
	Left	2.04	0.43 (21%)	0.18 (8.7%)	(7%–13%)	86%
Ratio						
Striatum-to-background	Bilateral	1.77	0.096 (5%)	0.058 (3.3%)	(3%–5%)	73%
	Right	1.78	0.10 (6%)	0.058 (3.3%)	(3%–5%)	76%
	Left	1.77	0.094 (5%)	0.063 (3.6%)	(3%–6%)	69%

*SDB = between-subject SD; SDW = within-subject SD; 95% CI = 95% confidence interval of SDW; and R = reliability coefficient.

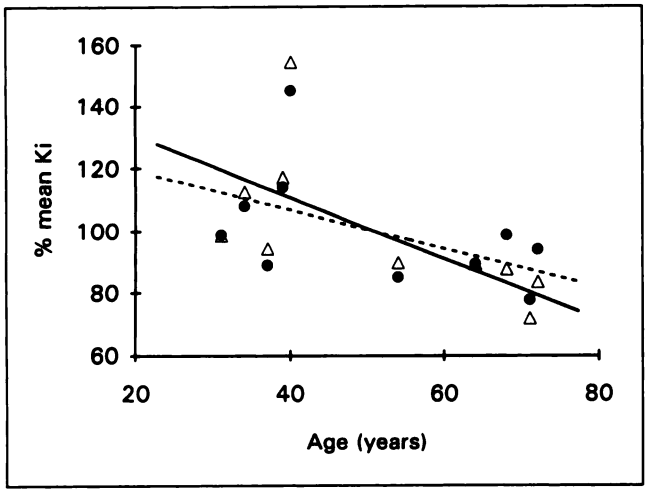

FIGURE 4. Age effect. Relationship between age and Ki from TS (△) or CP (●). For comparison, Ki values are given as a percentage of the population mean. The slope of the regression line for TS (—) is significant ($p = 0.048$) in contrast to the result for CP (– –) ($p = 0.15$).

from 77% to 83%. For background activity these values were respectively 7.2%–10.1%, 18%–20% and 78%–86% (Table 2).

Using the CP, the SDW of caudate activity varied between 7.6% and 11% at 25, 55, 85 and 115 min for the emission data. The SDB varied from 14% to 17% and the reliability from 63% to 80%. For the putamen activity, these values were respectively 7.3%–9.2%, 14%–18% and 69%–83%; and 7.5%–10.1%, 18%–22% and 80%–86% for background.

Blood Data

The mean SDW of PA, varied from 5.0% to 8.8% of the activity measured at 25, 55, 85 and 115 min. The SDB varied from 11% to 15% and reliability from 74% to 84%. For IPA, these values were respectively, 6.3%–7.8%, 10%–11% and 63%–76%. For θ the results were 3.4%–6.4%, 5%–7% and 43%–81%.

TABLE 2
Striatum and Blood Activities: Mean Values, Standard Deviations and Reliability Coefficients

Parameter	Time (min)	Mean	SDB (% of mean)	SDW (% of mean)	R
Emission TS					
Total striatum	25	2.12	0.33 (16%)	0.18 (8.6%)	77%
(10^3 MBq/ml)	55	2.26	0.39 (17%)	0.17 (7.6%)	83%
	85	2.18	0.39 (18%)	0.19 (8.6%)	81%
	115	2.04	0.37 (18%)	0.19 (9.4%)	79%
Background	25	1.83	0.33 (18%)	0.13 (7.2%)	86%
(10^3 MBq/ml)	55	1.49	0.27 (18%)	0.12 (7.8%)	84%
	85	1.21	0.22 (18%)	0.12 (9.9%)	78%
	115	1.03	0.21 (20%)	0.10 (10.1%)	80%
Emission CP Set					
Bilateral caudate	25	2.39	0.33 (14%)	0.25 (11%)	63%
(10^3 MBq/ml)	55	2.76	0.42 (15%)	0.21 (7.6%)	80%
	85	2.83	0.45 (16%)	0.27 (9.5%)	74%
	115	2.72	0.47 (17%)	0.28 (10.2%)	74%
Bilateral putamen	25	2.58	0.36 (14%)	0.24 (9.2%)	69%
(10^3 MBq/ml)	55	2.84	0.47 (16%)	0.21 (7.3%)	83%
	85	2.82	0.45 (18%)	0.24 (8.3%)	79%
	115	2.69	0.49 (18%)	0.23 (8.6%)	82%
Background	25	1.79	0.33 (18%)	0.13 (7.5%)	86%
(10^3 MBq/ml)	55	1.48	0.11 (19%)	0.11 (7.7%)	86%
	85	1.21	0.12 (20%)	0.12 (10.1%)	80%
	115	1.03	0.10 (22%)	0.10 (10.0%)	83%
Blood					
PA	25	548	61.8 (11%)	27.4 (5.0%)	84%
(counts/min)	55	392	52.1 (13%)	28.7 (7.3%)	77%
	85	321	45.8 (14%)	21.8 (6.8%)	82%
	115	275	40.7 (15%)	24.2 (8.8%)	74%
IPA	25	274	28.1 (10%)	21.3 (7.8%)	63%
(10^2 cts^2/min^2)	55	413	41.9 (10%)	27.1 (6.6%)	70%
	85	521	54.7 (10%)	33.7 (6.5%)	73%
	115	609	67.3 (11%)	38.3 (6.3%)	76%
θ (min)	25	50.1	3.64 (7%)	3.20 (6.4%)	56%
	55	106	7.33 (7%)	4.20 (3.9%)	76%
	85	163	11.5 (7%)	5.53 (3.4%)	81%
	115	223	12.0 (5%)	13.9 (6.2%)	43%

TABLE 3
Effect of Different Metabolite Correction on Final Ki (20–120 min) (10^{-1} ml min^{-1} $striatum^{-1}$)*

Metabolite correction	Side	Mean	SDB (% of mean)	SDW (% of mean)	95% CI	R
Measured						
	Bilateral	2.41	0.64 (26%)	0.21 (8.7%)	(7%–13%)	90%
	Right	2.43	0.61 (25%)	0.22 (9%)	(7%–14%)	89%
	Left	2.40	0.68 (28%)	0.22 (9.1%)	(7%–13%)	91%
Fixed (population sample mean)						
	Bilateral	2.41	0.61 (26%)	0.25 (10.6%)	(7%–13%)	85%
	Right	2.42	0.59 (24%)	0.26 (10.8%)	(9%–17%)	83%
	Left	2.39	0.64 (27%)	0.26 (10.8%)	(9%–17%)	86%

*SDB = between-subject SD; SDW = within-subject SD; 95% CI = 95% confidence interval of SDW; and R = reliability coefficient.

Metabolite Correction

The chi-square goodness of fit test yielded p values ranging from 0.935 to 1 (median: 0.999986) confirming the excellent linear fit of 3OMD/FD versus time.

The mean slope of 3OMD/FD versus time was 0.0621 min^{-1} (SDB of 16% and a SDW of 10.4%, reliability of 71%). The s.d. of duplicate analysis of this slope for each scan was 2% of the mean value (19.5% of SDW).

A fixed metabolite correction factor corresponding to the mean value of the population sample increased the SDW of Ki to 10.6% and reduced the reliability to 85% (Table 3).

Propagation of Error Variance

The net s.d. due to subjects, calculated from the variance component analysis, was 25% of the mean Ki. Variation in emission data gave a net s.d. of 1.3% when the TS was used. This contrasted with the 2.2% net s.d. from the metabolite correction and with 3.9% from blood data (Table 4).

DISCUSSION

We have shown that repeated FD PET in normal subjects yields reliability coefficients ranging from 73% to 90% depending upon the method of analysis. These results, with a SDW around 9%, contrast with those obtained from nonhuman primates where the SDW was 34.4% (*8*). This difference is probably mainly due to the higher human striatal volume and to the better resolution of the scanner used in the present study. Both decrease the effect of repositioning (*11*), which was probably a major source of variation in the nonhuman study (*8,21*). Correction of this source of error by back-to-back scanning in the nonhuman primates reduced the SDW to 14% (*8*) which is comparable to the present study. Another difference is that larger blood samples may be taken from humans, thus increasing the accuracy of blood analysis.

The analysis method directly affected the reliability. The ratio method was the most stable over time with a SDW representing only 3.3% of the mean, but it was also the least sensitive to between-subject differences (5%) leading to a reliability coefficient of 73%. Both graphical methods gave higher interindividual differences (SDB 22%–26%). This advantage outweighed the higher intraindividual variances (SDW 8.7%–10.3%) leading to a substantial improvement in the reliability of the results (R, 82%–90%). In addition to greater reliability, the graphical methods, based upon compartmental theories (*14,15*), more closely reflect the underlying physiological mechanisms (*22*).

Reliability of the results was affected by the ROI size (Fig. 2). This is partially due to decreased variation in emission counts with higher sampling. In addition, a ROI that encompasses the whole striatum will be less prone to degradation of data by subject movement. This is particularly important in many movement disorders. The method is also less sensitive to small differences in repositioning. As such, TS ROIs are a more objective measure of striatal activity and will give a higher reliability than the smaller CP (Table 2).

Another difference between the two graphical methods

TABLE 4
Net Standard Deviations of TS Ki Related to Subject and to the Three Components of the Graphical Analysis

	ml $striatum^{-1}$ min^{-1} (% of the population's Ki average)		
	Left	Right	Bilateral
Subject	0.058 (24%)	0.064 (27%)	0.061 (25%)
Emission	0.0032 (1.3%)	0.0035 (1.5%)	0.0031 (1.3%)
Blood	0.0092 (3.8%)	0.0097 (4.0%)	0.0094 (3.9%)
Metabolite	0.0054 (2.2%)	0.0053 (2.2%)	0.0053 (2.2%)

TABLE 5
Numbers of Subjects Needed in Each Group of a Parallel Study to Reach Significance (p = 0.05) With a Power of 80%

Methods	Observed difference in multiples of observed population s.d.								
	2	1.5	1.25	1	0.9	0.8	0.7	0.6	0.5
Graphical									
TS	1	2	3	4	5	6	8	11	15
CP putamen	1	2	3	4	5	7	8	11	16
CP caudate	2	2	3	5	6	7	9	12	17
Ratio	2	3	3	5	6	8	10	13	19

is that the TS measures total FD accumulation summed over the entire striatal volume while CP determines the uptake rate specific to each milliliter of striatal tissue. Because nigrostriatal dopaminergic function reflects the status of the substantia nigra (*23*), any change in volume of the striatum can inappropriately influence the Ki calculated from CP. A practical demonstration of this is the effect of age on nigrostriatal dopaminergic function. Using TS, an age-related decline in Ki is detected in our data (Fig. 4). That correlates well with the postmortem studies that show a decline in the number of nigral neurons (*24,25*). It has been shown elsewhere that striatal volume also decreases with age (*26*). This would increase the relative concentration of dopaminergic terminals (for the same number of dopaminergic neurons). This would spuriously increase the Ki calculated from the CP (Fig. 4).

A direct implication of this study is that it allows power calculations for prospective PET studies (Table 5). The aim of the planned study influences the choice of the method:

1. The ratio method, with the smallest SDW, may be best to assess natural evolution.
2. The TS method, taking into account peripheral dopa metabolism, will permit the use of smaller numbers of subjects for drug studies.
3. The CP method will identify regional changes, such as in the differential involvement of the caudate and the putamen in PD (*27*) at the risk of an increase in subject number.

Following FD injection, the labeled compounds present in the plasma of subjects pretreated with carbidopa are FD and 3OMFD (*17*). The ratio of 3OMFD/FD in plasma increases with time and may be modeled by a linear relationship during the first 2 hr following the injection. This is confirmed here by the high p values from the chi-square goodness of fit test. The slope of 3OMFD/FD versus time may be routinely and accurately measured as described by Chan et al. (*12,18*). This accuracy is confirmed in our study by the low variation between the duplicate measurements (s.d. 2%). In contrast, the SDW of the metabolite correction was 10.4%. This is probably due to physiological variations of COMT activity, as Ki reliability improved when measured metabolite correction was applied. This underlies the need for measured metabolite correction.

The blood activity, reflected by θ, had low reliability (Table 2). The results at 25 and 115 min, which are weighted by their position at the endpoints of the graphical analysis, have particularly low reliability of 56% and 43%, respectively. The early result is influenced mainly by the estimation of IPA. An explanation for the low early reliability is the rapid variation in PA during the first minutes following a bolus of FD which may not be accurately evaluated even by fast blood sampling. Automated blood sampling or slower administration of FD may decrease this effect and deserves further evaluation. In contrast, the low reliability of θ at 115 min is due to decreasing reliability of the measurement of PA. This is probably due to the low count rate of ^{18}F after one half-life. The impact of any measurement inaccuracy in the measured PA is compensated by the fact that it forms the denominator of both axes of the graphical method. Thus, the SDW and R of Ki remain stable even when calculation of Ki is continued from 85 to 115 min (Table 1). This extension of the calculation decreased the Ki. This probably reflected a loss of 6-[^{18}F]-fluorodopamine from the final compartment (*14,15*).

Variation in blood data had the greatest influence on the final Ki (Table 4). This represented 50% more than the contribution of the metabolite correction and three times more than the contribution of the emission data. Refining the blood activity measurement should produce the greatest improvement in reproducibility of FD PET data.

CONCLUSION

We have shown that FD PET yields reproducible results with reliability coefficients between 73% and 90%, depending on the method of ROI analysis used. Graphical analysis with TS gave the most reliable result. This is the best method for examining a generalized effect on the nigrostriatal dopaminergic system. The CD ROIs gave less reliable results and are potentially perturbed by a change in striatal volume; their application should be reserved for intrastriatal comparisons. The need for accurate correction for peripheral metabolism of FD is emphasized. Blood data are the least reliable component of the analysis; further evaluation is needed to improve the accuracy of this component. The data presented in this paper form the basis for assessing the significance of changes detected in FD PET studies of human subjects and for power analysis in the planning of longitudinal studies.

ACKNOWLEDGMENTS

The authors thank Brian Pate for his valuable advice and support; and Grace Chan, Poppy Shofield, Patrick Hooper and the TRIUMF group for their help in performing the PET scans. This study was supported by the Medical Research Council of Canada, the National Parkinson Foundation and the Dystonia Medical Research Foundation.

REFERENCES

1. Bhatt M, Snow BJ, Martin WRW, Pate BD, Ruth TJ, Calne DB. Positron emission tomography suggests that the rate of progression of idiopathic parkinsonism is slow. *Ann Neurol* 1991;29:673–677.
2. Laihinen A, Rinne JO, Rinne UK, et al. Fluorine-18-6-fluorodopa PET scanning in Parkinson's disease after selective COMT inhibition with nitecapone (OR-462). *Neurology* 1992;42:199–203.
3. Holden JE, Pate BD, Snow BJ, et al. Effects of simultaneous inhibition of MAO-B and COMT on striatal L-6-fluorodopa kinetics in nonhuman primates [Abstract]. *Sixth symposium on the medical application of cyclotrons.* Turku, Finland; 1992.
4. Guttman M, Burns RS, Martin WRW, et al. PET studies of parkinsonian patients treated with autologous adrenal transplants. *Can J Neurol Sci* 1989;16:305–309.
5. Sawle GV, Bloomfield P, Bjorklund A, et al. Transplantation of fetal dopamine neurons in Parkinson's disease: PET [^{18}F]-6-L-fluorodopa studies in two patients with putaminal implants. *Ann Neurol* 1992;31:166–173.
6. Widner H, Tetrud JW, Rehncrona S, et al. Bilateral fetal mesencephalic grafting in two patients with parkinsonism induced by 1-methyl-4-phenyl-1,2,3,6-tetrahydropyridine (MPTP). *N Engl J Med* 1992;327:1556–63.
7. van Belle G, Uhlmann RF, Hughes JP, Larson EB. Reliability of estimates of changes in mental status test performance in senile dementia of the Alzheimer type. *J Clin Epidemiol* 1990;43:589–595.
8. Pate BD, Snow BJ, Hewitt KA, Morrison KS, Ruth TJ, Calne DB. The reproducibility of striatal uptake data obtained with positron emission tomography and fluorine-18 L-6-fluorodopa tracer in non-human primates. *J Nucl Med* 1991;32:1246–1251.
9. Powers WJ, Berg L, Perlmutter JS, Raichle ME. Technology assessement revisited: does positron emission tomography have proven clinical efficacy? *Neurology* 1991;41:1339–1340.
10. Therapeutics and Technology Assessement Subcommittee. Assessement: positron emission tomography. *Neurology* 1991;41:163–167.
11. Sossi V, Buckley KR, Ruth TJ. Effect of axial (2 D mode) sampling resolution on striatal phantom imaging in an ECAT 953/B compared to a PET VI [Abstract]. *Proc Conf IEEE* 1993;885–887.
12. Chan GLY, Hewitt KA, Pate BD, Schofield P, Adam MJ, Ruth TJ. Routine determination of [^{18}F]-L-6-fluorodopa and its metabolites in blood plasma is essential for accurate positron emission tomography studies. *Life Sci* 1991; 50:309–318.
13. Martin WRW, Palmer MR, Patlak CS, Calne DB. Nigrostriatal function in man studied with positron emission tomography. *Ann Neurol* 1989;26:535–542.
14. Patlak CS, Blasberg RG. Graphical evaluation of blood-to-brain transfer constants from multiple-time uptake data. Generalizations. *J Cereb Blood Flow Metab* 1985;5:584–590.
15. Patlak CS, Blasberg RG, Fenstermacher JD. Graphical evaluation of blood-to-brain transfer constants from multiple-time uptake data. *J Cereb Blood Flow Metab* 1983;3:1–7.
16. Scheffé H. *The analysis of variance.* New York: Wiley & Sons; 1959:221–260.
17. Boyes BE, Cumming P, Martin WRW, McGeer EG. Determination of plasma ^{18}F-fluorodopa during positron emission tomography: elimination and metabolism in carbidopa treated subjects. *Life Sci* 1986;39:2243–2252.
18. Chan GLY, Morrison KS, Holden JE, Ruth TJ. Plasma L-[18F]6-fluorodopa input function: a simplified method. *J Cereb Blood Flow Metab* 1992; 12:881–884.
19. Dunn DJ, Clark VA. *Applied statistics: analysis of variance and regression,* 2nd edition. New York: Wiley & Sons; 1987:214–235.
20. Fleiss JL. *The design and analysis of clinical experiments.* New York: Wiley & Son; 1986:8–14.
21. Links JM. The influence of positioning on accuracy and precision in emission tomography. *J Nucl Med* 1991;32:1252–1253.
22. Carson RE. Precision and accuracy considerations of physiological quantitation in PET. *J Cereb Blood Flow Metab* 1991;11:A45–A50.
23. McGeer ED, Calne DB, Snow BJ, Tooyama I, Takahashi H, Yamada T. Correlation of postmortem striatal dopamine levels with nigral cell counts and uptake of ^{18}F-fluorodopa in premortem PET scans [Abstract]. *Soc Neurosci* 1992;18:665.
24. McGeer PL, McGeer EG, Suzuki JS. Aging and extrapyramidal function. *Arch Neurol* 1977;34:33–35.
25. Gibb WRG, Lees AJ. Anatomy, pigmentation, ventral and dorsal subpopulations of the substantia nigra, and differential cell death in Parkinson's disease. *J Neurol Neurosurg Psychiatr* 1991;54:388–396.
26. Murphy DGM, DeCarli C, Schapiro MB, Rapoport SI, Horwitz B. Age-related differences in volumes of subcortical nuclei, brain matter, and cerebrospinal fluid in healthy men as measured with magnetic resonnance imaging. *Arch Neurol* 1992;49:839–845.
27. Brooks DJ, Ibanez V, Sawle GV, et al. Differing patterns of striatal [^{18}F]-dopa uptake in Parkinson's disease, multiple system atrophy, and progressive supranuclear palsy. *Ann Neurol* 1990;28:547–555.

EDITORIAL

PET Studies in Psychiatry: Validity, Accuracy and Future

PET with its high resolution and array of ligands again demonstrates its vitality and power in the series of preceding papers which illustrate its reproducibility, clinical utility and value in understanding metabolic function.

Degeneration of nigral dopaminergic neurons of the caudate nucleus, putamen and globus pallidus underlies the pathogenesis of Parkinson's disease with its characteristic movement disorders. Fluorine-18-L-6-fluorodopa (FD) is a substrate for the enzymes involved in L-dopa metabolism. FD is converted to fluorodopamine. In normal subjects, FD accumulates within the striatum. In patients with Parkinson's disease, striatal uptake is reduced. As an important index of nigro-striatal dopaminergic function, FD uptake has been used in studies of schizophrenia, Parkinson's disease and intracerebral transplantation of adrenal and fetal tissue.

Dr. Vingerhoets and coworkers (*1*) address an important issue of intra-subject and intersubject variations in striatal uptake of FD. They observed that FD-PET yields reproducible results with reliability coefficients between 73%–90%. They made an important and significant observation that variation in blood radioactivity contributed to the variability of Ki more than metabolite correction. However, separation of FD from its metabolites is essential for each FD-PET scan. This study demonstrates that PET measurements in normal subjects are stable across repeated scans, a finding indicative of wide normal variation in dopaminergic function which lends credence to recent risk studies.

Received Nov. 4, 1993; accepted Nov. 4, 1993.
For correspondence or reprints contact: Shankar Vallabhajosula, PhD, Div. of Nuclear Medicine, Dept. of Radiology, Mount Sinai Medical Center, One Gustave L. Levy Pl., New York, NY 10029-6574.